Leveraging MIMO Transmit Diversity for Channel-Agnostic Device Identification

Nora Basha[†], Bechir Hamdaoui[†], Kathiravetpillai Sivanesan[‡]
[†] Oregon State University, Corvallis, OR, USA; Email: {bashano,hamdaoui}@oregonstate.edu
[‡] Intel Corporation, Hillsboro, OR, USA; Email: kathiravetpillai.sivanesan@intel.com

***Abstract*— The accurate identification of wireless devices is critical for enabling automated network access monitoring and authenticated data communication in large-scale networks; e.g., IoT networks. RF fingerprinting has emerged as a potential solution for device identification by leveraging the transmitter unique manufacturing impairments of the RF components. Although deep learning is proven efficient in classifying devices based on the hardware impairments, trained models perform poorly due to channel variations. That is, although training and testing neural networks using data generated during the same period achieve reliable classification, testing them on data generated at different times degrades the accuracy substantially. To the best of our knowledge, we are the first to propose to leverage MIMO capabilities to mitigate the channel effect and provide a channel-resilient device classification. For the proposed technique we show that, for Rayleigh channels, blind partial channel estimation enabled by MIMO increases the testing accuracy by up to 40% when the models are trained and tested over the same channel, and by up to 60% when the models are tested on a channel that is different from that used for training.**

I. Introduction

As the IoT paradigm is pervasively expanding into critical sectors including healthcare, home automation, and power grids, the flux of insecure devices connected to the Internet is increasing the risk of attacks on IoT networks [1], [2]. Therefore, verifying the identity of the devices to prevent illegitimate devices from accessing and exploiting the network resources using an identification technique that is immune to spoofing and light enough to be implemented on the resource-constrained IoT devices is becoming crucial. RF data-driven device fingerprinting has emerged as a promising technique for identifying and classifying devices using physical-level features that are much difficult, if not impossible, to spoof or replicate. Transceiver hardware impairments that are inevitably inherited during device manufacturing provides a fingerprint for each device that, unlike high-layer features such as IP or MAC addresses, is immune to spoofing. Those hardware imperfections impair the transmitted waveforms in a way that provides transmitters with fingerprints and signatures that can uniquely separate them from one another [3], [4].

Deep learning–or precisely Deep Neural Network (DNN)–based approaches have proven efficient in classifying devices from captured RF signals due to the DNNs' high dimensional mapping and ability to process data without the need of hand-crafted feature extraction. However, the often considered assumption that the training and testing data exhibit identical distribution causes DNN-based RF fingerprinting model accuracy to drastically degrade due to the time- and/or location-varying wireless channel conditions that invalidate such an assumption [5]–[7]. In addition, the channel overshadows device fingerprints causing difficulties in training new models in the presence of fading and impairments.

In this paper, we propose a novel, channel-resilient device fingerprinting technique that tackles the wireless channel effect on DNN-based RF fingerprinting by leveraging the MIMO capabilities in mitigating flat fading in Rayleigh channels. We show that Blind Channel Estimation performed by leveraging the MIMO capabilities combined with STBC (Space Time Block Coding) improves the training accuracy by 40% over Rayleigh flat fading channel compared to conventional SISO systems. We also show that when trained and tested under different flat fading channels, the accuracy of the DNN model is improved by up to 60% compared to SISO systems.

The rest of the paper is organized as follows. Section II presents previous related works. Section III provides some background on blind channel estimation and presents the proposed technique. Section IV presents simulation results and evaluation. Finally, Section V concludes the paper.

II. Related Works

Experimental results [5], [7] showed that channel condition variations severely degrade the fingerprinting accuracy, dropping it from 85% to 10% on WiFi data. In an effort to address these challenges, Sankhe *et al.* [3] exploited the configuration flexibility of SDRs to modify the transmitter chain so as to increase device separability and fingerprinting robustness to channel variations. Likewise, Restuccia *et al.* [8] showed that a carefully-optimized digital finite input response filter at the transmitter's side can improve the accuracy from about 40% to about 60%. However, these works modify the transmitted signals by either adding artificial impairments that are channel immune, or by filtering to alter the transmitted signals to maximize the model accuracy. In addition, these techniques require changes to be made at the transmitters' side.

Unlike these works, Elmaghbub *et al.* [4], [6], [9] proposed a new fingerprinting technique that improves fingerprinting accuracy without requiring changes to be made at the devices. The basic idea lies in leveraging spectrum emissions in the band surrounding the signal's original band that are caused by various transceiver hardware impairments to increase device distinguishability and robustness to channel variations.

In this work, we propose a new framework that leverages MIMO capabilities to mitigate the channel effect also without the need for altering the transmitted signals, impacting the BER, nor modifying the hardware. To the best of our knowledge, we are the first to suggest leveraging MIMO capabilities to mitigate channel effect on RF fingerprinting. Our proposed technique relies on blind partial channel estimation, enabled by MIMO and STBC, to overcome the impact of channel distortions on the training and testing of the deep learning models, thereby improving the robustness of device classification to changes in channel conditions.

III. Leveraging MIMO for Channel-Agnostic Wireless Device Identification

A. Background on MIMO and Blind Channel Estimation

MIMO (Multiple-Input Multiple-Output) links improve SNR (signal-to-noise ratio) of multipath fading channels through spatial diversity by combining the output signals received on the multiple uncorrelated elements of the antenna arrays [10]. The SNR improvement achieved through diversity is characterized by: (i) Array gain, which measures the increase in average output SNR relative to the single antenna average SNR. (ii) Diversity gain, which measures the increase in the error rate slope as a function of the SNR [10].

STBC (Space Time Block Coding) is a coding technique that achieves transmit diversity by spreading information symbols in space using multiple transmitting antennas and in time using pre-coding [10], [11]. Spreading in space and time is achieved by an $M \times K \quad (K \leq M)$ code matrix $\mathcal{C}$, where K is the time diversity of the code and M is the number of transmitting antennas. Each column i of $\mathcal{C}$ corresponds to the signals transmitted by all the transmitting antennas at time epoch i, $1 \leq i \leq K$. For instance, the code matrix $\mathcal{C}$ of the Alamouti scheme [12] (with two transmit antennas) is

$$\mathcal{C} = \begin{bmatrix} c_1 & -c_2^* \\ c_2 & c_1^* \end{bmatrix}$$

where c_1 and c_2 are the symbols transmitted (each on one of the two transmit antennas) at the the first time epoch, and $-c_2^*$ and c_1^* are the symbols transmitted at the second time epoch. When the receiver is equipped with one antenna only, Alamouti scheme does not achieve an array gain. However, for i.i.d. Rayleigh channels, a diversity gain is achieved and the symbol error rate is reduced. To achieve array gain, the receiver must be equipped with more than one antenna.

When sending an STBC data matrix $\mathbf{S}$ using an $M \times L$ MIMO system over a flat fading channel, the received signal matrix after K time epoch is given by:

$$\mathbf{R} = (\mathbf{I}_K \otimes \mathbf{H})\mathbf{C}\mathbf{S} + \mathbf{N} \tag{1}$$

where $\mathbf{C} = \begin{bmatrix} \mathbf{C}_1^T & \mathbf{C}_2^T & \ldots & \mathbf{C}_K^T \end{bmatrix}^T$, $\mathbf{C_k}$ is a matrix calculated from the code matrix $\mathcal{C}$ for $k = 1, \ldots, K$, $\mathbf{H}$ is the channel matrix, $\mathbf{N}$ is the noise matrix, and $\otimes$ denotes the Kronecker product operation [13], [14].

STBCs enable the blind estimation of the channel by observing only the received signals [13], [14]. Eq. (1) shows that, for a MIMO system transmitting an STBC signal over a flat fading channel, each receiving antenna receives a signal that is a mixture of the signals transmitted by all the transmitting antennas, and each of the transmitted signals contributes to the mixture with a weight dictated by the channel matrix. The problem of estimating the transmitted signals given only the received signals and the properties of the transmitted signals, referred to as the blind source separation/blind channel estimation problem, essentially boils down to finding the inverse of the channel matrix, which can then be used to recover the transmitted signals [13]–[15]. The recovered transmitted signals are less affected by the channel and are expected to achieve higher classification accuracy compared to the unprocessed received signals when used for RF fingerprinting.

The blind estimation algorithm in [13], [14] aims at determining the subspace of the channel matrix. First, the algorithm starts by finding $\mathbf{N}_L$, the left null space of $\mathbf{R}$. Eq. (1) yields the following blind equation [13], [14]

$$\mathbf{N}_L^H(\mathbf{I}_K \otimes \mathbf{H})\mathbf{C} = \mathbf{0} \tag{2}$$

which represents a homogeneous linear equation in the unknown $\mathbf{H}$, and the uniqueness of the solution depends on the matrix $\mathbf{C}$ of the STBC and the rank of the matrix $\mathbf{H}$ as explained in [13], [14]. Second, the blind algorithm decouples the channel matrix subspace from Eq. (2) to get:

$$\overbrace{(\sum_{k=1}^{K} \mathbf{C}_k^T \otimes (\mathbf{N}_L^H \mathbf{E}_k))}^{\triangleq \boldsymbol{\Delta}} \mathbf{h} = 0 \quad \text{with } \mathbf{E}_k \triangleq \begin{bmatrix} \mathbf{0}_{L(k-1)\times L} \\ \hline \mathbf{I}_L \\ \hline \mathbf{0}_{L(K-k)\times L} \end{bmatrix} \tag{3}$$

Eq. (3) shows that channel subspace, $\mathbf{h}$, lies in the null space of $\boldsymbol{\Delta}$. Yet, the actual channel cannot be identified from its rotated versions due to the remaining complex ambiguity [14].

B. The Proposed MIMO-Enabled Device Fingerprinting

For Rayleigh flat fading channels, the channel conditions (i.e., the channel matrix $\mathbf{H}$) impact the transmitted waveforms causing an accuracy degradation of trained classification models. The received signal by each of the receiving antennas is a mixture of the signals transmitted by all the transmitting antennas. Estimating the transmitted signals given the received signals and the properties of the transmitted signals could be achieved via blind source separation/blind channel estimation methods, which remove the channel effects on the transmitted signals without the need for training pilots. In this work, we propose to use blind partial channel estimation enabled by MIMO [14] to estimate the subspace of the channel matrix from the received signal matrix given the STBC used for transmission. If the estimated channel subspace is used to reconstruct the originally transmitted signal, the reconstructed transmitted signal is expected to be less affected by the channel impairments, and the effect of the channel is less when the number of remained ambiguities is minimized. To guarantee the minimum ambiguity in the estimated channel matrix, i.e. a single complex ambiguity in the estimated channel, we use a 3×3 MIMO system that transmits a QPSK signal using Tarokh STBC of rate $1/2$ (code length = 8) [14]. A single complex ambiguity is interpreted as an unknown scaling factor, and such a factor is expected to have a minor effect on the classification accuracy. We exploit Convolution Neural Network (CNN) high dimensional feature mapping capabilities and high performance in classifying RF devices to achieve accurate classification from the reconstructed transmitted signals despite the remaining ambiguities.

At the transmitter side, each 80 symbols are modulated using QPSK, then the modulated symbols are encoded into blocks using Tarokh STBC of rate $1/2$ (code/block length = 8) such that each transmitted block encodes 4 QPSK modulated symbols. For 20 transmitted blocks, we construct the STBC symbol matrix $\mathbf{S}$ with size of 24×20, where the columns represent the transmitted blocks from the 3 transmitting antennas. The signals transmitted by each of the transmitting antennas are obtained by reshaping $\mathbf{S}$ into a 3×160 matrix $\mathcal{S}$. Each row in $\mathcal{S}$ represent the signal transmitted by each of the 3 transmitting antennas. The transmitted signals are then impaired by MIMO Rayleigh fading. The channel is fixed for 20 transmitted blocks. At the receiver side, we first apply the blind algorithm [14] to determine the channel matrix subspace as explained in Section III-A. To construct the matrix $\mathbf{\Delta}$, we first collect 20 received blocks from the 3 receiving antennas in a matrix $\mathcal{R}$ with the size of 3×160, then we construct the matrix $\mathbf{R}$ for the received STBC blocks. R is a 24×20 matrix, where the columns represent the received blocks from the 3 receiving antennas. To calculate the left null space N_L of the received signal matrix $\mathbf{R}$, we use Singular Value Decomposition (SVD), $\mathbf{R} = \mathbf{U}\mathbf{\Sigma}\mathbf{V}^H$, where $\mathbf{U}$ and $\mathbf{V}$ are complex unitary square matrices with the size of 24, and 20 respectively. Since each transmitted block has the length of 8, rank($\mathbf{R}$) is also 8. Thereby, the left null space of R, N_L, is spanned by the columns of U starting from column number 9. Matrix $\mathbf{C_k}$ is determined by the STBC used from transmission. The channel subspace $\mathbf{h}$, which is the right null space of $\mathbf{\Delta}$, is then calculated using SVD of matrix $\mathbf{\Delta}$, $\mathbf{\Delta} = \mathbf{U}'\mathbf{\Sigma}'\mathbf{V}'^H$, and the right null space of $\mathbf{\Delta}$, i.e. the estimated channel subspace, is the column of $\mathbf{V}'$ corresponding to the smallest singular value (the last column of $\mathbf{V}'$).

Second, we reconstruct the transmitted signals, $\hat{\mathcal{S}}$, using the inversion of the estimated channel subspace as $\hat{\mathcal{S}} = \mathbf{H}^{\dagger}\mathcal{R}$, where $\{.\}^{\dagger}$ denotes the pseudoinverse. The reconstructed transmitted signals $\hat{\mathcal{S}}$ are then sampled with a window size of 160 for each of simulated devices to create the training, validation, and testing datasets. The reconstructed transmitted signals $\hat{\mathcal{S}}$ are less affected by the fading channel, and hence are expected to achieve higher accuracy compared to the raw IQ data when used to train and test the CNN models. The reconstructed signals are also expected to be more immune to the channel condition variations when used for classifying devices using previously trained CNN models on a varying channel conditions.

IV. Performance Evaluation and Analysis

We use MATLAB R2020b to build our wireless communication model and generate the IQ datasets. The IQ data were collected form 10 simulated RF devices uniquely impaired with the impairments set shown in Table I. The impairments are set slightly different to mimic the slight differences among devices. For each device, we collected 5000 frames, with each frame having the size of 160. Then we split the real and the imaginary parts of the signal and reshaped the frames as 2×160 vectors to be fed to the input layer of the CNN. The dataset was divided into 80% for training, 10% for validation and 10% for testing.

A. CNN Architecture

We used the CNN architecture in [3] as a benchmark to evaluate the proposed MIMO-enabled approach, study its resiliency, and compare it to the SISO/conventional approach. The CNN architecture consists of two convolution layers and two fully connected layers. The 2×160 input is fed into the first convolution layer that consists of 50 1×7 filters. This layer produces 50 features maps from the entire input. The second convolution layer consists of 50 $2{\times}7$ filters, where each filter is convoluted with the 50-D volumes obtained from the first layer. The second convolution layer learns variations over both I and Q dimensions. Each convolution layer is followed by a ReLU activation function to add non-linearity, and a 2-stride max pooling layer to prevent overfitting. The first fully connected layer consists of 256 nodes whose output are fed into the second fully connected layer of 80 nodes. Each fully connected layer has a ReLU activation. The last layer is a soft max classifier to generate the classification probabilities. At the classifier output, the cross-entropy loss is calculated and the back-propagation algorithm is used to find the network parameters that minimize the prediction error. The CNN uses Adam optimizer.

B. Performance Metrics

We consider the following metrics in this evaluation.

- **Training Accuracy/Testing Accuracy**, the percentage of the correctly classified samples to the total number of samples in the training/testing datatsets.
- **Relative Different channel Testing Gap (RDTG)**, the percentage of reduction occurred in the testing accuracy when the testing and testing channels are different. Precisely, RDTG is defined as

$$\text{RDTG} = \frac{\text{same channel testing acc.} - \text{different channel testing acc.}}{\text{same channel testing acc.}} \%$$

  When the classification technique is perfectly channel-agnostic, then RDTG is zero, and the deviation from zero quantifies the effect of the channel variation on accuracy.

In the evaluation of the proposed fading channel-agnostic technique, we also vary the following parameters:

- **Training APG/Testing APG**, the average path gain (APG) of the Rayleigh flat fading channel used for training/testing. APG is varied from -20 dB to 20 dB.

TABLE I
HARDWARE IMPAIRMENTS USED TO SIMULATE 10 DIFFERENT DEVICES

Device	Phase Noise	Frequency Offset	IQ Gain Imbalance	IQ Phase Imbalance	AMAM	AMPM	Real DC Offset	Imaginary DC Offset
DV1	-60	20	0.08	0.1	[2.1587,1.1517]	[4.0033,9.104]	0.1	0.15
DV2	-60.15	20.01	0.1	0.09	[2.1687,1.1617]	[4.1033,9.124]	0.11	0.14
DV3	-59.9	20.2	0.09	0.09	[2.1789,1.1317]	[4.0933,9.151]	0.1	0.11
DV4	-60.1	20	0.108	0.109	[2.1987,1.1217]	[4.1033,9.194]	0.1	0.1
DV5	-60	20.09	0.1	0	[2.1587,1.1717]	[4.093,9.094]	0.089	0.1008
DV6	-59.95	20.1	0.12	0.15	[2.1487,1.1117]	[4.1033,9.156]	0.1	0.098
DV7	-59.93	20.11	0.11	0.11	[2.1897,1.1237]	[4.1133,9.135]	0.111	0.1011
DV8	-60.13	20.099	0.101	0.14	[2.1387,1.1627]	[4.1533,9.096]	0.12	0.099
DV9	-59.89	19.9	0.099	0.08	[2.1548,1.1917]	[4.09833,9.10056]	0.09	0.0999
DV10	-59.91	19.98	0.111	0.105	[2.1777,1.09874]	[4.0987,9.123]	0.101	0.10015

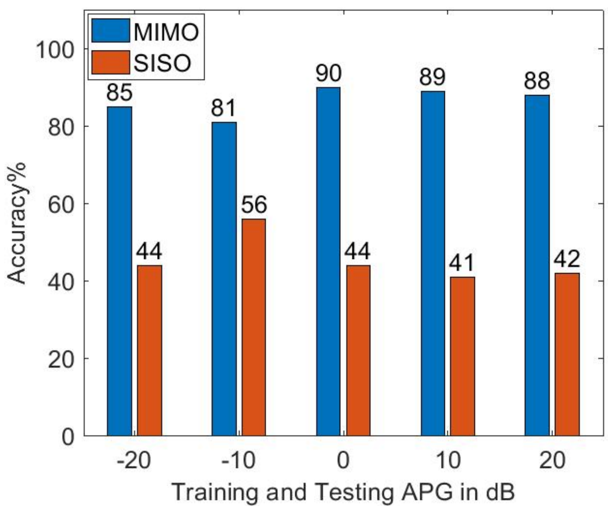

Fig. 1. Same Rayleigh channel is used for training and testing.

C. Simulation Results

In order to ensure that the flat fading channels are blindly identifiable from the received signal only, without feedback from the receiving end to the transmitting devices, as explained in Section III, we simulate and collect data from 10 devices each using a 3×3 MIMO system to send QPSK symbols encoded via Tarokh STBC $\mathcal{O}_3$ [11]. The transmitted signal blocks are impaired with a flat fading Rayleigh MIMO channel. At the receiving end, blind partial channel estimation is performed and the reconstructed signals are used for training and testing the CNN model. For fair comparison, we assume that there is no feedback from the receiving end to the transmitting devices in the conventional/SISO approach.

1) Training and Testing Over the Same Rayleigh Channel: In this section, we analyze the results obtained when training and testing are performed over the same Rayleigh fading channel for both MIMO and SISO approaches. Figure 1 shows the obtained testing accuracy while varying the APG. This figure clearly shows that the proposed MIMO-enabled approach increases the testing accuracy significantly compared to the conventional/SISO approach. For instance, we observe that at training and testing APG of -20 dB, the MIMO-enabled approach increases the testing accuracy from 44% to up to 85% compared to the SISO approach, thereby doubling the obtained accuracy. In addition, we observe that the accuracy improvement that MIMO-enabled approach offers over the conventional approach is consistent across the entire APG value range, i.e., our proposed MIMO-enabled classification approach doubles the accuracy regardless of the APG value.

2) Training and Testing Over Different Rayleigh Channels: This scenario mimics real world settings where the classification models are trained under certain channel conditions, but then used later for real-time device classification under different channel conditions.

a) Testing Accuracy Performance: Figure 2 shows the testing accuracy over Rayleigh channels where the models are trained and tested over channels with different APG values, ranging from 20 to -20 dB. This figure shows the effect of the wireless channel on the device classification accuracy. For instance, we observe that for the conventional/SISO method (Figure 2e), the models achieve an accuracy of about 44% when trained and tested over a (same) channel with training and testing APG of -20 dB. However, these same models only achieve about 18% when trained over a channel with APG = -20 dB but tested over a channel with APG = 20 dB. Our observation indicating the seriousness of the channel impact on device classification accuracy is well aligned with previous work findings as discussed in Sections I and II. The figure also shows that the proposed MIMO-enabled approach significantly improves the testing accuracy over the conventional/SISO approach when the training channels exhibit severe fading. In addition, we observe that the MIMO-based approach testing accuracy is more stable when the CNN is trained at severe fading channels. Looking at Figure 2a, which depicts the testing accuracy achieved under varied APG values of the testing channel at a fixed training APG of 20 dB, we observe that for testing APG greater than 0 dB, MIMO achieves improved performance over SISO. However, when the testing APG is less than 0 dB, the testing accuracy is unreliable, and both SISO and MIMO approaches are equivalent. For instance, when the testing APG is 10 dB, the MIMO-based approach achieves a testing accuracy of about 52%, but only about 23% is achieved under the conventional/SISO approach. However, when the testing APG is -10 dB, both MIMO and SISO approaches provide severely degraded and unreliable testing accuracy.

Now in Figure 2b, which depicts the testing accuracy under varied APG values of the testing channel at a fixed training APG of 10 dB, we observe that the MIMO-based approach achieves significant higher testing accuracy compared to the

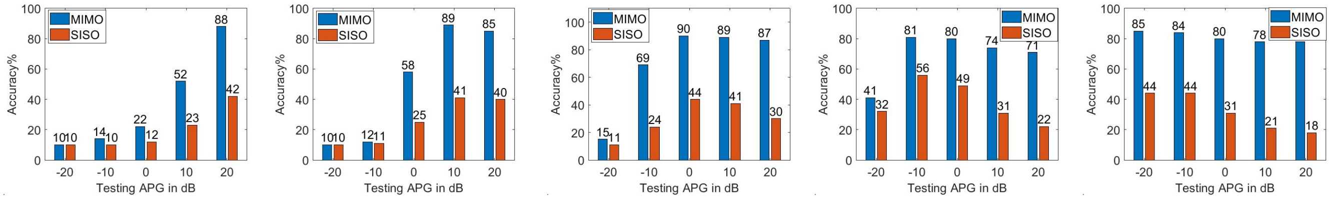

(a) Training APG = 20dB (b) Training APG = 10dB (c) Training APG = 0dB (d) Training APG = -10dB (e) Training APG = -20dB

Fig. 2. Impact of APG on accuracy.

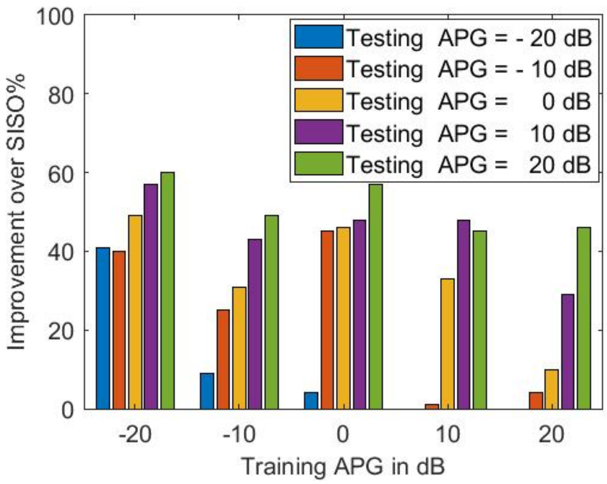

Fig. 3. Impact of Training APG on the MIMO improvement over SISO under flat fading Rayleigh channels

SISO approach when the testing APG is greater than 0 dB. For instance, when the training APG is 10 dB and the testing APG is 20 dB (channel with less severe fading), MIMO system achieves a testing accuracy of about 85%, whereas only about 40% is achieved under SISO. Moreover, when the testing APG = 0 dB (channel with more severe fading), the testing accuracy improves from 25% to about 58% when considering the MIMO-based approach versus the SISO approach. Figure 2c and Figure 2d show the same trends observed in Figure 2b. Figure 2e captures the testing accuracy when varying the testing APG values at a fixed training APG of -20 dB. From this figure we first observe that when testing on different channels with testing APG values varying from -10 dB to 20 dB, the MIMO-based classification approach achieves an improved and stable testing accuracy when compared to the SISO approach. For instance, when the training APG is -20 dB and the testing APG is 20 dB, the MIMO approach achieves up to 60% increase in the testing accuracy over the SISO approach. Second, when the training APG is -20 dB (severe fading channel), the testing accuracy of the MIMO approach at different channels with testing APG varying from -10 dB to 20 dB does not go below 78% compared to the SISO approach where the testing accuracy degrades to 18%.

Figure 3 illustrates the improvement/gain in testing accuracy that the MIMO-based approach achieves over the SISO approach when the CNN is trained and tested under various different APG values, ranging from 20 dB to -20 dB. From this figure we first observe that when the CNN is trained on severe fading channel with training APG of -20 dB, the MIMO-based approach shows significant improvement over the conventional/SISO approach, and when the CNN is trained on less severe fading channels, i.e. training APG values higher than -20 dB, the improvement over the SISO approach decreases. For instance, an improvement of up to 60% in the MIMO approach performance is achieved when the training APG is -20 dB and the testing APG values varies from -10 dB to 20 dB. However, when the training APG is -10 dB, the MIMO improvement decreases to 50%. This could be justified by the severely degraded testing accuracy for the SISO system over severe fading channels. Second, we observe that when the CNN is trained at less severe fading channels with training APG values varying from 0 dB to 20 dB and tested at severe fading channels with testing APG values less than -10 dB, the MIMO system improvement over SISO vanishes. Third, we observe that when the CNN is trained on severe fading channels then tested on less severe fading channels, the MIMO-based approach shows significantly improved performance over the SISO approach. Note that when the training APG is -10 dB and the testing APG is 10 dB, MIMO achieves about 43% improvement over SISO, compared to only 9% improvement when the testing APG is -20 dB.

b) RDTG Performance: We now assess the robustness of the proposed MIMO-enabled fingerprinting approach against Rayleigh channel condition variations through the study of the RDTG performance metric introduced in Section IV-B. Figure 4 shows RDTG values when training and testing of the learning models are done over Rayleigh channels with varying APG values. First, observe that compared to the SISO approach, the MIMO-based approach provides a much higher resiliency to channel variations, i.e. yields smaller RDTG values, when the training channel exhibits moderate (training APG = 0 dB; Figure 4c) to severe (training APG = -20 dB; Figure 4e) fading conditions. One explanation for this observation is that despite the MIMO-enabled blind estimation, the remaining ambiguity in the estimated channel affect the learning models in the training phase, where the models still learn features that are extracted from both channel and device impairments. Therefore, training at less severe flat

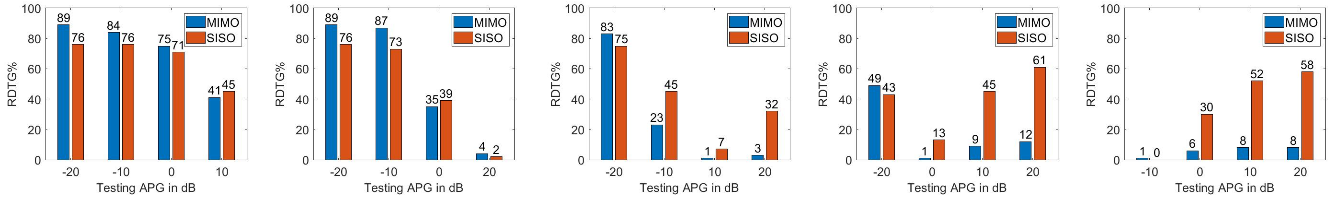

(a) Training APG = 20dB (b) Training APG = 10dB (c) Training APG = 0dB (d) Training APG = -10dB (e) Training APG = -20dB

Fig. 4. Impact of APG on RDTG.

fading channels while testing at more severe fading channels yields significant reduction in the accuracy. However, the MIMO-based approach still outperforms the SISO approach in spite of this unsolved ambiguity. Observe that the closer the testing APG values are to the training ones, the smaller the RDTG values achieved under MIMO are. This observation is commensurate with the previous observations made in Figure 2 about the MIMO-based approach testing accuracy degradation when tested on more severe fading channels.

Now when considering moderate training APGs like 0 dB as in Figure 4c, we observe that the MIMO-based approach is less immune to the channel variation when tested on a channel that is significantly more severe than that used for training. For instance, when testing APG = -20 dB, the RDTG value achieved under the MIMO-based approach is 83%. However, the higher the testing APG, the lesser the RDTG value; i.e., the more resilient the MIMO-enabled approach is to channel condition variations. Figure 4e, depicting RDTG values when the training APG = -20 dB, shows that when the fading conditions of the training channel become worse, the SISO approach continues to degrade significantly, but not so for the proposed MIMO approach. Moreover, as the testing APG continues to increase, while the MIMO-based approach maintains stable RDTG values (about 8%), SISO performance continues to degrade significantly, reaching RDTG values of up to 58%.

V. Conclusion

In this work we propose a deep learning-based MIMO-enabled RF/device classification approach, and showed that the MIMO capabilities can indeed mitigate the wireless channel effect and improve the RF fingerprinting accuracy for Rayleigh flat fading channel. We showed that the proposed MIMO-based approach improves the classification accuracy by up to 60% compared to the conventional/SISO approach, and that the improvement the MIMO approach achieves over the conventional approach is more significant and stable when the model is tested on less severe fading channels compared to the channel used for training.

Acknowledgment

This work was supported in part by the US National Science Foundation under NSF award No. 1923884 and NSF/Intel No. 2003273.

References

[1] A. Rachedi, M. H. Rehmani, S. Cherkaoui, and J. J. P. C. Rodrigues, "IEEE Access Special Section Editorial: The Plethora of Research in Internet of Things (IoT)," *IEEE Access*, vol. 4, 2016.

[2] J. Bao, B. Hamdaoui, and W.-K. Wong, "IoT device type identification using hybrid deep learning approach for increased IoT security," in *2020 International Wireless Communications and Mobile Computing (IWCMC)*. IEEE, 2020, pp. 565–570.

[3] K. Sankhe, M. Belgiovine, F. Zhou, S. Riyaz, S. Ioannidis, and K. Chowdhury, "ORACLE: Optimized Radio clAssification through Convolutional neuraL nEtworks," in *IEEE INFOCOM 2019 - IEEE Conference on Computer Communications*. IEEE, 2019.

[4] A. Elmaghbub, B. Hamdaoui, and A. Natarajan, "Widescan: Exploiting out-of-band distortion for device classification using deep learning," in *GLOBECOM 2020-2020 IEEE Global Communications Conference*. IEEE, 2020.

[5] A. Al-Shawabka, F. Restuccia, S. D'Oro, T. Jian, B. Costa Rendon, N. Soltani, J. Dy, S. Ioannidis, K. Chowdhury, and T. Melodia, "Exposing the Fingerprint: Dissecting the Impact of the Wireless Channel on Radio Fingerprinting," in *IEEE INFOCOM 2020 - IEEE Conference on Computer Communications*, 2020.

[6] B. Hamdaoui, A. Elmaghbub, and S. Mejri, "Deep neural network feature designs for RF data-driven wireless device classification," *IEEE Network*, vol. 35, no. 3, pp. 191–197, 2020.

[7] A. Elmaghbub and B. Hamdaoui, "Comprehensive RF dataset collection and release: A deep learning-based device fingerprinting use case," in *2021 IEEE Globecom Workshops (GC Wkshps)*. IEEE, 2021, pp. 1–6.

[8] F. Restuccia, S. D'Oro, A. Al-Shawabka, M. Belgiovine, L. Angioloni, S. Ioannidis, K. Chowdhury, and T. Melodia, "DeepRadioID: Real-Time Channel-Resilient Optimization of Deep Learning-based Radio Fingerprinting Algorithms," *arXiv:1904.07623 [cs]*, 2019.

[9] A. Elmaghbub and B. Hamdaoui, "LoRa device fingerprinting in the wild: Disclosing RF data-driven fingerprint sensitivity to deployment variability," *IEEE Access*, 2021.

[10] B. Clerckx and C. Oestges, *MIMO Wireless Networks : Channels, Techniques and Standards for Multi-Antenna, Multi-User and Multi-Cell Systems*. Elsevier Science & Technology, 2013.

[11] V. Tarokh, H. Jafarkhani, and A. Calderbank, "Space-time block codes from orthogonal designs," *IEEE Transaction on Information Theory*, vol. 45, no. 5, 1999.

[12] S. Alamouti, "A simple transmit diversity technique for wireless communications," *IEEE Journal on Selected Areas in Communications*, vol. 16, no. 8, 1998.

[13] N. Ammar and Zhi Ding, "On blind channel identifiability under space-time coded transmission," in *Conference Record of the Thirty-Sixth Asilomar Conference on Signals, Systems and Computers, 2002.*, vol. 1, 2002.

[14] N. Ammar and Z. Ding, "Blind Channel Identifiability for Generic Linear Space-Time Block Codes," *IEEE Trans. Signal Process.*, vol. 55, no. 1, 2007.

[15] A. Hyvärinen, J. Karhunen, and E. Oja, *Independent Component Analysis*. S.l: Wiley-Interscience, 2001, oCLC: 845874768.